α-Fe_2O_3
Preparation by Sol-Gel Method

Lab Manual

M.Sc Physics (Sem III)
Nanoscience Lab

By: Manas Sharma
manassharma07@live.com
University of Delhi

October 14, 2017

1 Objective

To prepare α-Fe_2O_3 nanoparticles by sol-gel technique and study the effect of different annealing temperatures and heating times on the crystallite size using the peak widths of the diffractograms(XRD) of the differently prepared samples.

2 Theory

2.1 Nanoscience

Nano refers to the order 10^{-9}. It means one billionth of something. Nano can be ascribed to any unit of measure. For example, one may report a very small mass in nanograms or the amount of liquid in one cell in terms of nanoliters. So, what is nanoscience? Nanoscience is the study of structures and materials on the scale of nanometers. To give you an idea of how long a nanometer is, this printed page is about 75,000 nanometers thick. When structures are made small enoughin the nanometer size rangethey can take on interesting and useful properties.
Nanoscale structures have existed in nature long before scientists began studying them in laboratories. A single strand of DNA, the building block of all living things, is about three nanometers wide. The scales on a morpho butterflys wings contain nanostructures that change the way light waves interact with each other, giving the wings brilliant metallic blue and green hues. Peacock feathers and soap bubbles also get their iridescent coloration from light interacting with structures just tens of nanometers thick. Scientists have even created nanostructures in the laboratory that mimic some of natures amazing nanostructures.

2.2 Nanoscale architecture(fabrication)

Because nanostructures are so small, specialized methods are needed to manufacture objects in this size range. Nanotechnology is the design, fabrication and use of nanostructured systems, and the growing, shaping or assembling of such systems either mechanically, chemically or biologically to form nanoscale architectures, systems and devices. The original vision of Richard Feynman was of the bottom-up approach of fabricating materials and devices at the atomic or molecular scale, possibly using methods of self-organization and self-assembly of the individual building blocks. An alternative top-down approach is the ultraminiaturization or etching/milling of smaller structures from larger ones. Both approaches require a means of visualizing, measuring and manipulating the properties of nanostructures; computer-based simulations of the behaviour of materials at these length scales are also necessary. This chapter provides a general introduction to the preparation and properties of nanostructures, whilst the subsequent chapters give greater detail on specific topics.

Figure 1: Morpho butterfly

Figure 2: Peacock Feather

Table 1: Examples of systems of different dimensions

3D confinement
Fullerenes
Colloidal particles
Nanoporous silicon
Activated carbons
Nitride and carbide precipitates in high-strength low-alloy steels
Semiconductor particles in a glass matrix for non-linear optical components
Semiconductor quantum dots (self-assembled and colloidal)
Quasi-crystals
2D confinement
Carbon nanotubes and nanofilaments
Metal and magnetic nanowires
Oxide and carbide nanorods
Semiconductor quantum wires
1D confinement
Nanolaminated or compositionally modulated materials
Grain boundary films
Clay platelets
Semiconductor quantum wells and superlattices
Magnetic multilayers and spin valve structures
LangmuirBlodgett films
Silicon inversion layers in field effect transistors
Surface-engineered materials for increased wear resistance or corrosion resistance

2.3 α-Fe_2O_3 (Hematite)

Hematite (αFe_2O_3) is one of the most important, stable, non-toxic, nature-friendly and corrosion-resistant metal oxides. It is an n-type semiconductor with optical bandgap (E_g) of 2.1 eV and possesses extensive applications in pigments, magnetic devices and as anticorrosive agents, catalysts, gas sensors and as photoanodes for photo-assisted electrolysis[8, 9]. The conduction band (CB) is composed of empty d-orbitals of Fe3+ and the valence band (VB) consists of fully occupied 3D crystal field orbitals of Fe3+ with some admixture from the O 2p nonbonding orbitals.[7] Hematite crystallizes in the hexagonal lattice system, and it has the same crystal structure as corundum(Al_2O_3). Fe_2O_3 has many other phases like $\beta - Fe_2O_3$, $\epsilon - Fe_2O_3$, $\gamma - Fe_2O_3(maghemite)$, but $\alpha - Fe_2O_3$ is the most stable of all the phases.

2.3.1 Structural Properties

- Crystal System: Trigonal
- Lattice type: Hexagonal
- Space Group: $R\bar{3}c$
- Color: black to steel or silver-gray, brown to reddish brown, or red

Lattice Parameters:

- $a = b = 5.035$Å
- $c = 13.748$Å
- $\alpha = \beta = 90^o$
- $\gamma = 120^o$.

One can visualize the α-Fe_2O_3 crystal by downloading and opening this CIF(Crystallographic Information File)[2] using a visualizing software like VESTA[5].

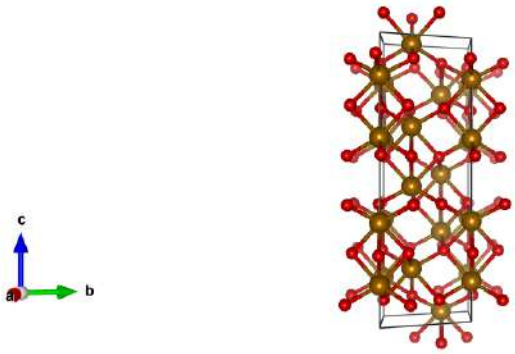

Figure 3: View along: $\vec{a}$

Figure 4: View along: $\vec{c}$

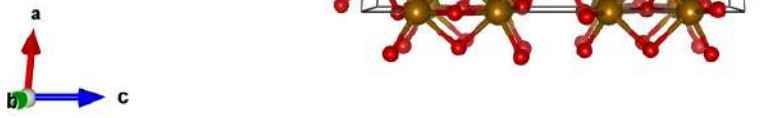

Figure 5: View along: $\vec{b}$

The following is a theoretical simulation of the powder XRD of α-Fe_2O_3 performed using VESTA.

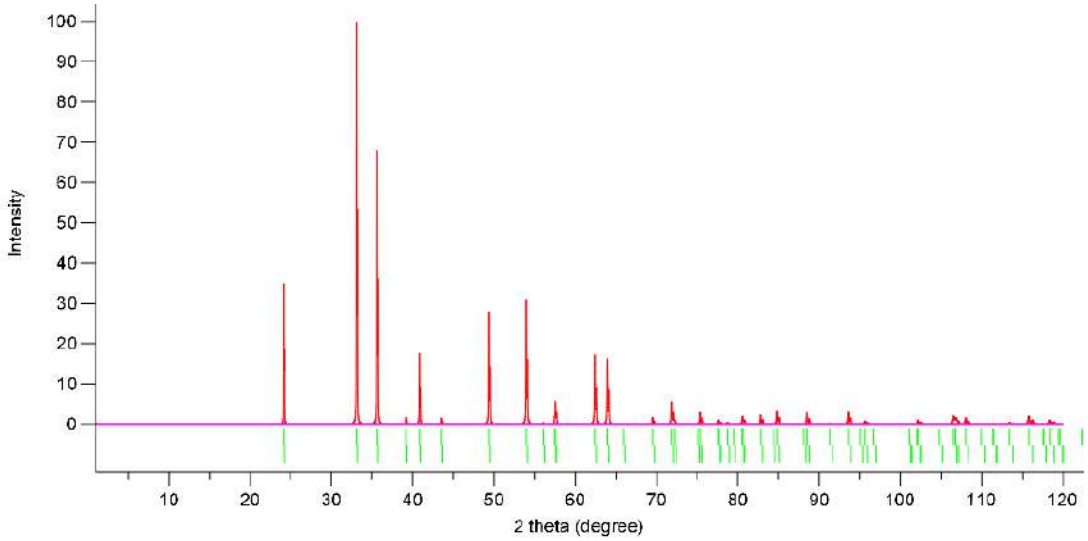

Figure 6: Powder XRD Simulation for α-Fe_2O_3

α-Fe_2O_3 behaves as an n-type semiconductor and also has a magnetic nature, as seen in the following DFT(Density Functional Theory) simulations of band structure and DOS(Density of states)[10].

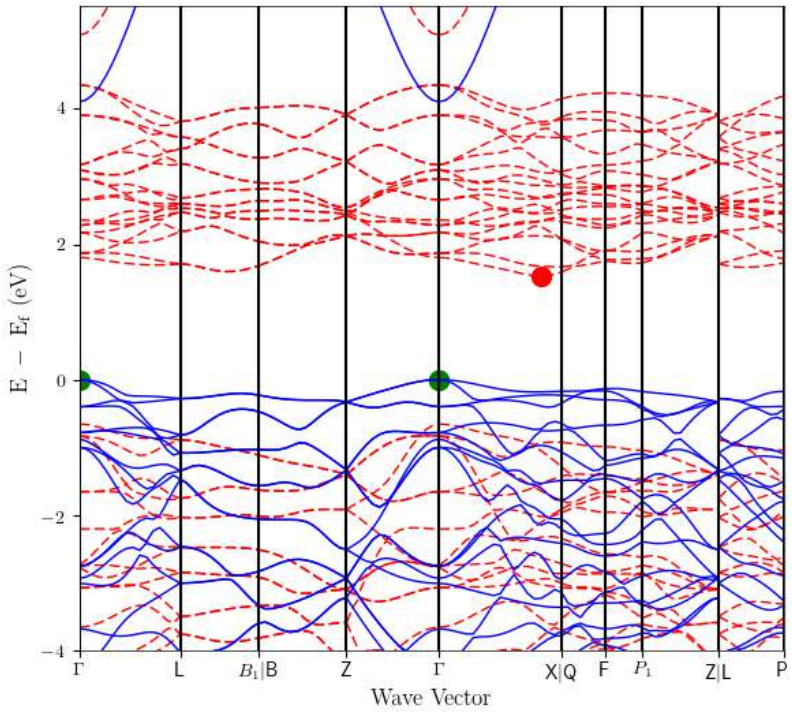

Figure 7: Band Structure

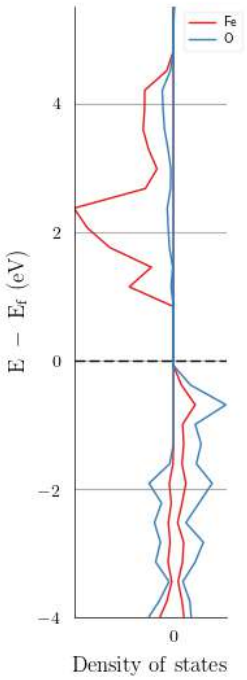

Figure 8: Density of States(DOS)

2.3.2 Magnetic Properties

Hematite is an antiferromagnetic material below the Morin transition at 250 kelvin (K) or -9.7 degrees Fahrenheit (F), and a canted antiferromagnet or weakly ferromagnetic above the Morin transition and below its Neel temperature at 948 K, above which it is paramagnetic. The magnetic structure of a-hematite was the subject of considerable discussion and debate in the 1950s because it appeared to be ferromagnetic with a Curie temperature of around 1000 K, but with an extremely tiny magnetic moment (0.002 μ_B).

2.3.3 Applications

Various applications of iron oxides in nano form can be attributed to the difference in behaviour of particles in nano scale as compared to their bulk counterparts. The nano particles usually have much larger surface area due to their smaller size and can reduce the volume required to achieve same effect when used as a catalyst.

- **Photo-electrochemical devices**
  Due to it's optical band gap, α-Fe_2O_3 has potential for use as a photoanode, for photoelectrochemcial devices. Moreover, since the band gap increases as one goes down in size into the nanoscale, therfore, nanoparticles of α-Fe_2O_3 are of special interest. Fe-based nano compounds as positive cathode materials for Li-ion secondary batteries are of interest due to the low-cost and non-toxicity. It has been observed that the enhancement in the polaronic conductivity nearly two orders in magnitude while reducing the crystallite size from bulk into nano scale level. The enhancement in the conductivity is due to the augmented to compressive strain developed in the material which leads to pronounced decrease in the hopping length of polarons. Thus, nanocrystaline α-Fe_2O_3 may be a better alternative anode material for lithium ion batteries than earlier reported systems.[1]

- **Pigments (coloring and coating material)**
  The use of hematite as a red/black pigment has been practised since pre-historic times. The anti-corrosive properties of hematite, make it suitable for use as pigments or coating material for steel construction and cars. By reducing the particle size to nano range(2-10nm), transparent iron oxide pigments can be obtained. Now a days such transparent iron oxide pigments are preferably used. These have good stability to temperature, and can resist up to 300^oC. These are strong absorbers of ultraviolet radiation and mostly used in automotive paints, wood finishes, construction paints, industrial coatings, plastic, nylon, rubber and print ink.

- **Magnetic Applications**
  If the size of the hematite nanoparticles is reduced to below a few nanometers, they become superparamagnetic. When a magnetic field is applied, the particles acquire a certain magnetization but, because of the high thermal energy, the long range order is lost when the field is removed, and the particles have no remnant magnetization.

2.4 Sol-Gel Technique

The sol-gel process is a method for producing solid materials from small molecules. The method is usually used for the fabrication of metal oxides.
In sol gel process initially a stable colloidal solution called sol is formed. The sol is a liquid suspension of solid particles ranging in size from 1 nm to 1 micron. It can be obtained by hydrolysis and partial condensation of precursors such as an inorganic salt or a metal alkoxide. Hydrolysis is a chemical reaction or process in which a chemical compound is broken down by reaction with water. The further condensation of sol particles into a three dimensional network produces a gel material. The gel is a diphasic system, that is they contain both liquid and solid phases.

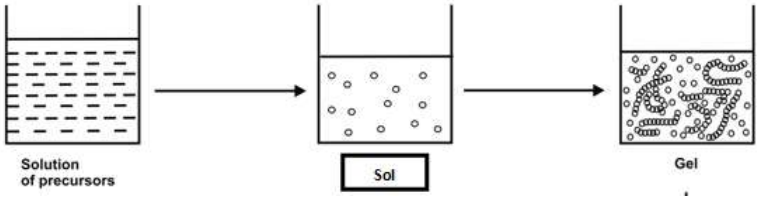

Figure 9: Sol-gel Process Schematic

Removal of the remaining liquid (solvent) phase requires a drying process, which is typically accompanied by a significant amount of shrinkage and densification. The rate at which the solvent can be removed is ultimately determined by the distribution of porosity in the gel. The ultimate microstructure of the final component will clearly be strongly influenced by changes imposed upon the structural template during this phase of processing.
Afterwards, a thermal treatment, or firing process, is often necessary in order to favor further polycondensation and enhance mechanical properties and structural stability via final sintering, densification and grain growth. One of the distinct advantages of using this methodology as opposed to the more traditional processing techniques is that densification is often achieved at a much lower temperature.

2.4.1 Advantages of sol-gel method

- Versatile: better control of the structure, including porosity and particle size; possibility of incorporating nanoparticles and organic materials into sol-gel-derived oxides;
- Extended composition ranges: it allows the fabrication of any oxide composition, but also some non-oxides, as well as the production of new hybrid organic-inorganic materials, which do not exist naturally;
- Better homogeneity: due to mixing at the molecular level; high purity;
- Less energy consumption: there is no need to reach the melting temperature, since the network structure can be achieved at relatively low temperatures;
- Coatings and thin films, monoliths, composites, porous membranes, powders and fibers;
- No need for special or expensive equipment.

2.5 X-Ray Diffraction

X-ray diffraction(XRD) is an important technique for determining the structures of crystals. The theory behind XRD is a result of pioneering works of the Braggs(father and son).
The main principle behind XRD is the diffraction of X-rays in specific directions by atoms in crystalline structure. Since the interplanar distances in crystals are of the order of Angstroms, therefore X-rays are the suitable choice, as the wavelength of the wave should be of the order of the slit size for the phenomenon of diffraction to take place.

Braggs suggested that the crystal structure can be considered as an array of atoms forming several planes. The X-rays on striking an atom will scatter in some direction. The scattered X-rays can interfere constructively if they are in phase or destructively if they are out of phase. Have a look at the following figure.

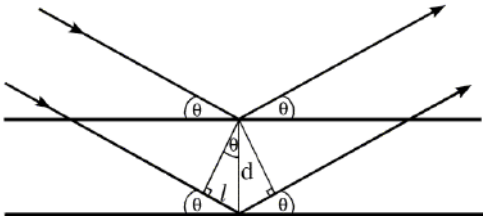

Figure 10: Bragg Planes

The path difference between the two X-rays scattering from the two planes can be easily seen to be $2d\sin\theta$ where d is the interplanar spacing and θ is the incident angle.
For the waves to interfere constructively, they should satisfy the following relation

$$2d\sin\theta = n\lambda$$

This is the Bragg's Law. Here, λ is the wavelength of the X-ray beam. Therefore the path difference between the X-rays scattered from two planes should be an integer multiple of the wavelength.
Essentially, we consider the crystal to be a diffraction grating for an X-ray.

XRD pattern: A simple X-ray diffraction experimental setup requires the following: a radiation source, a sample crystal, and a detector. These are arranged as shown in the given figure.

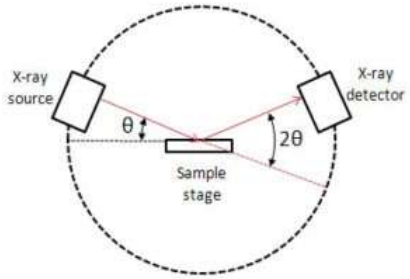

Figure 11: X-Ray Diffractometer schematic

The source gives off X-rays that strike the crystal at some angle θ, and the detector detects the scattered radiation, at angle of 2θ from the source. The X-rays hit the atoms in the crystal plane and scatter in different directions. For diffraction to occur, the scattered radiation must be coherent(in phase), therefore the scattering must be elastic. The angular position of the source is varied over the range of interest and correspondingly the detector, and the intensities of the scattered radiations are recorded and plotted versus 2θ. This plot of intensity of the scattered radiaiton vs 2θ is known as an XRD pattern. (Alternatively, sample can be rotated.)The detector can be of several kinds. It can be a simple photographic plate or a sophisticated Geiger/Scintillation counter. The intensity of the highest peak is set to 100 and the rest of the peaks are scaled with respect to this. Then the peaks are mapped to a particular set of lattice planes given by the corresponding miller indices. This is done by calculating the interplanar spacing(d) corresponding to a particular peak. And then using a relation between d and the (hkl) indices for different lattice types:

Cubic:

$$\frac{1}{d^2} = \frac{h^2+k^2+l^2}{a^2}$$

Tetragonal:

$$\frac{1}{d^2} = \frac{h^2+k^2}{a^2} + \frac{l^2}{c^2}$$

Hexagonal:

$$\frac{1}{d^2} = \frac{4}{3}\left(\frac{h^2 + hk + k^2}{a^2}\right) + \frac{l^2}{c^2}$$

Rhombohedral:

$$\frac{1}{d^2} = \frac{(h^2 + k^2 + l^2)\sin^2\alpha + 2(hk + kl + hl)(\cos^2\alpha - \cos\alpha)}{a^2(1 - 3\cos^2\alpha + 2\cos^3\alpha)}$$

Orthorhombic:

$$\frac{1}{d^2} = \frac{h^2}{a^2} + \frac{k^2}{b^2} + \frac{l^2}{c^2}$$

Monoclinic:

$$\frac{1}{d^2} = \left(\frac{h^2}{a^2} + \frac{k^2\sin^2\beta}{b^2} + \frac{l^2}{c^2} - \frac{2hl\cos\beta}{ac}\right)\csc^2\beta$$

Triclinic:

$$\frac{1}{d^2} = \frac{\frac{h^2}{a^2}\sin^2\alpha + \frac{k^2}{b^2}\sin^2\beta + \frac{l^2}{c^2}\sin^2\gamma + \frac{2kl}{bc}\cos\alpha + \frac{2hl}{ac}\cos\beta + \frac{2hk}{ab}\cos\gamma}{1 - \cos^2\alpha - \cos^2\beta - \cos^2\gamma + 2\cos\alpha\cos\beta\cos\gamma}$$

Generally, a crystal would consist of many planes oriented in different directions. When X-rays strike the crystal at an angle θ to a particular plane, then if this angle, satisfies the Bragg's law, then we would get an intensity peak corresponding to that particular plane in the XRD pattern. All the parallel planes contribute to a particular peak. If the incident angle of X-rays is changed to different values, then we may or may not get intensity peaks in the XRD pattern corresponding to the different planes depending on whether they satisfy the Bragg's law or not.

The following are some of examples of the XRD pattern that one obtains:

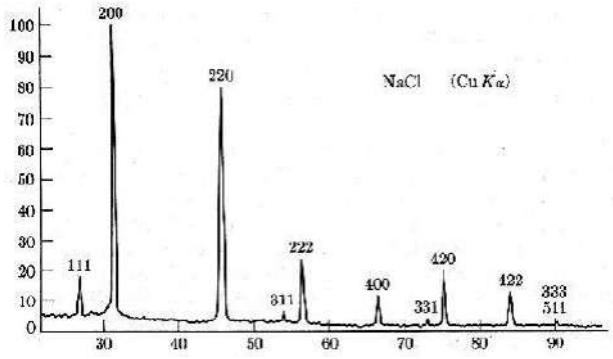

Figure 12: Diffractogram of NaCl (fcc structure)

2.6 Peak height, Peak width and Crystallite size

Bragg's equation tells us about the position of the peaks, but it doesn't give any information about the intensity(height) of the peaks. To understand the scattering of x-rays from a crystal, we need to consider the following:

- Scattering from electrons
- Scattering from atoms
- Scattering from a unit cell

Peak height, loosely called the intensity, can generally be attributed to the density of atoms in a plane. Overall, the following factors affect the peak height:

- Polarization factor due to scattering from electrons

- Atomic scattering factor due to scattering from atoms
- Structure Factor due to scattering from unit cell

Structure Factor defines the resultant wave scattered by all atoms of the unit cell. The Structure Factor is independent of the shape and size of the unit cell; but is dependent on the position of the atoms/ions etc. within the cell.

Ideally, one should get sharp lines in the XRD pattern. However, practically, one gets lines of finite width. The broadening of the peaks is caused by a number of factors. The following are the factors that affect the width of the peaks:

- Crystallite size
- Instrumental Profile
- Crystal defects and strain
- Temperature

The peak widths can therefore,be used to calculate the crystallite size of the sample. Scherrer gave a relation between the peak width and crystallite size in 1918:

$$\beta(2\theta) = \frac{K\lambda}{L\cos\theta}$$

where β is the peak width in radians, which depends on 2θ. The peak width is usually taken to be the FWHM(Full width at half maximum) or the integral breadth(area under the peak divided by the peak height). L is the crystallite size and K is the Scherrer constant, that depends on the how the width is determined, the shape of the crystal, and the size distribution.
The most common values for K are:

- 0.94 for FWHM of spherical crystals with cubic symmetry
- 0.89 for integral breadth of spherical crystals w/ cubic symmetry
- 1, because 0.94 and 0.89 both round up to 1

K actually varies from 0.62 to 2.08.
λ is the wavelength of the X-Ray used.
θ is the peak position in degrees. Thus, one can clearly see that the crystallite size is inversely proportional to the peak width. However,one should note that the Scherrer equation is limited to nano-scale particles and can't be used for particles greater than 100nm.
The peak width also varies with 2θ. The crystallite size broadening is most pronounced at large angles 2θ. However, the instrumental profile width and microstrain broadening are also largest at large angles 2θ. Moreover,peak intensity is usually weakest at larger angles 2θ. Therfore one often gets better results from using diffraction peaks between 30^o and 50^o 2θ.

3 Procedure

3.1 Preparation of samples

We will prepare two samples of α-Fe_2O_3 nanoparticles. Sample a will be annealed at 550^oC for 20 hrs and sample b will be annealed at 900^oC for 10 hrs

1. Prepare a 0.1M Ferric Nitrate solution to be used as precursor.
2. To do that take, 8.08g of $Fe(NO_3)_3.9H_2O$ as solute and ethanol as solvent to prepare a solution of 200ml.
3. Now heat the solution at around 60^oC with vigourous stirring using a magnetic stirrer for around 20 hrs until just 10ml of the solution remains.

$$Fe(NO_3)_3.9H_2O \rightarrow Fe_2O_3 + 5H_2O + 6HNO_3$$

4. The remaining solution is then dried at 200^{o}C.
5. Finally the dried powder is annealed at very high temperature(500^o − 900^{o}C) for 10-20 hrs.
6. After the nanoparticles are prepared, perform a powder X-Ray diffraction and compare it with a standard database to confirm the phase.
7. Find out the interplanar spacings of the various planes, and calculate the lattice parameters.
8. Also calculate the crystallite size using Scherrer equation.

3.2 Calculating FWHM using ORIGIN[6]

1. Zoom into the peak whose FWHM is to be determined.
2. Go to Analysis->Peaks and Baseline->Multiple Peak Fit->Open dialog
3. Select Gaussian Peak Function from the drop down menu.
4. Select the peak, whose Gaussian Fit is to be found, by double clicking on it's tip.
5. Click on the fit until converge button and note down the value of FWHM.

4 Observations

4.1 Diffractograms:

The powder XRD patterns of both the samples using Cu K_α rays of wavelength, $\lambda = 1.541$Å are shown below.
Sample prepared at 550^o C and annealed for 20hrs.

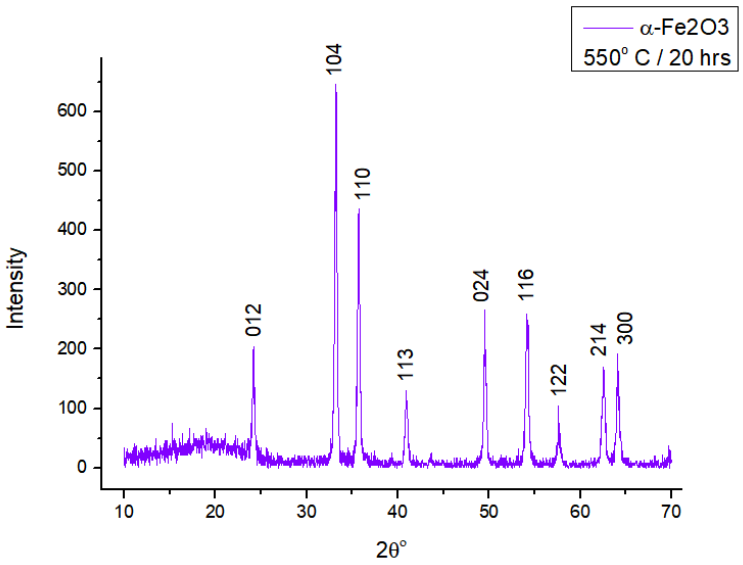

Figure 13: Diffractogram of Sample a

Sample prepared at 900^o C and annealed for 10hrs.

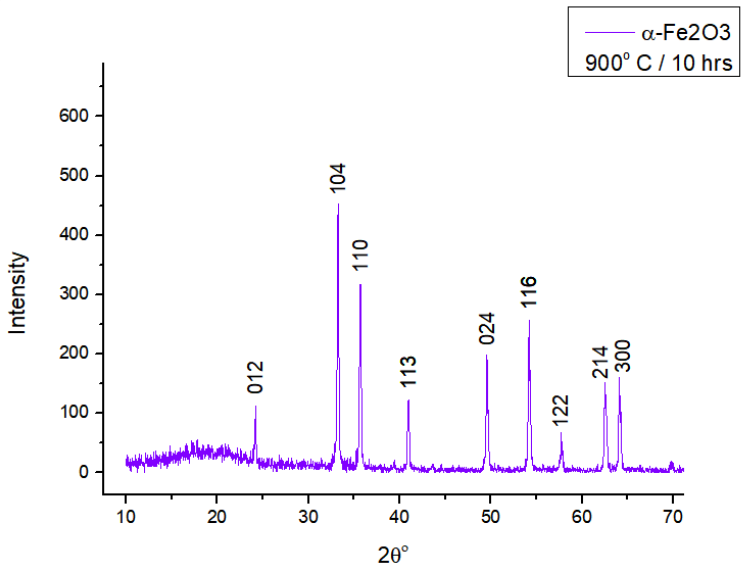

Figure 14: Diffractogram of Sample b

Sample prepared at 600^o C and annealed for 48hrs.

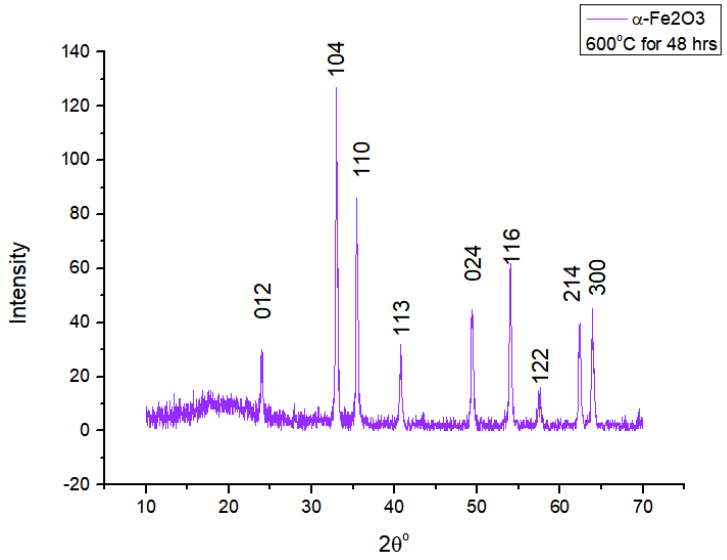

Figure 15: Diffractogram of Sample c

Sample prepared at 800^o C and annealed for 10hrs.

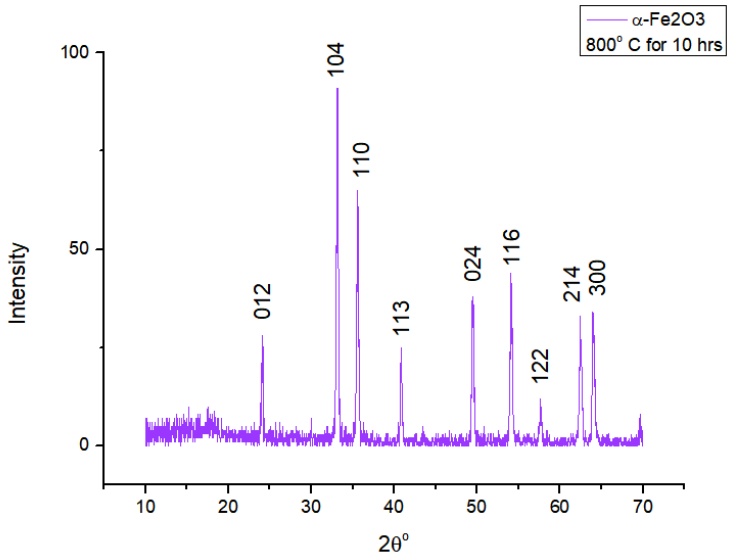

Figure 16: Diffractogram of Sample d

4.2 Color

- Sample prepared at 550^o C and annealed for 20 hrs was **REDDISH BROWN** in color.
- Sample prepared at 600^o C and annealed for 48 hrs was **REDDISH BROWN** in color.
- Sample prepared at 800^o C and annealed for 10 hrs was **METALLIC GREY** in color.
- Sample prepared at 900^o C and annealed for 10 hrs was **METALLIC GREY** in color.

4.3 Interplanar spacings d_{hkl}

Interplanar spacings can be calculated using,

$$d = \frac{\lambda}{2\sin\theta}$$

Sample a (550^o C / 20 hrs):

Table 2: Interplanar spacings of the various peaks

Peak position $2\theta(^o)$	Peak position $2\theta(rad)$	$2\sin\theta$	d_{hkl} (Å)	hkl	JCPDS(d_{hkl})
24.106	0.42073	0.41764	3.6917	012	3.6840
33.201	0.57946	0.57139	2.6983	104	2.7000
35.688	0.62288	0.61286	2.5157	110	2.5190
40.923	0.71424	0.69916	2.2052	113	2.2070
49.547	0.86476	0.83807	1.8397	024	1.8406
54.166	0.94538	0.91056	1.6932	116	1.6941
57.615	1.0056	0.96373	1.5998	122	1.6033
62.596	1.0925	1.0390	1.4839	214	1.4859
64.190	1.1203	1.0626	1.4509	300	1.4543

Sample b (900^o C / 10 hrs):

Table 3: Interplanar spacings of the various peaks

Peak position $2\theta(^o)$	Peak position $2\theta(rad)$	$2\sin\theta$	d_{hkl} (Å)	hkl	JCPDS(d_{hkl})
24.179	0.42201	0.41888	3.6807	012	3.6840
33.201	0.57946	0.57139	2.6983	104	2.7000
35.688	0.62288	0.61286	2.5157	110	2.5190
40.951	0.71472	0.69961	2.2038	113	2.2070
49.547	0.86476	0.83807	1.8397	024	1.8406
54.166	0.94538	0.91056	1.6932	116	1.6941
57.712	1.0073	0.96522	1.5973	122	1.6033
62.533	1.0914	1.0380	1.4853	214	1.4859
64.054	1.1179	1.0606	1.4536	300	1.4543

4.4 Calculating Lattice Parameters

The relation relating the lattice parameters to the interplanar spacing for the Hexagonal structure is:

$$\frac{1}{d^2} = \frac{4}{3}\left(\frac{h^2+hk+k^2}{a^2}\right) + \frac{l^2}{c^2}$$

Sample a(550^oC for 20hrs):

For the peak(110) at $2\theta = 35.688^o$:

$$d = 2.5157\text{Å}$$

For this peak,

$$a = 2d$$
$$\implies \boxed{a = 5.0314\text{Å}}$$

For the peak(113) at $2\theta = 40.923^o$:

$$d = 2.2052\text{Å}$$

We have already calculated

$$a = 5.0314\text{Å}$$

Using this,

$$\implies \boxed{c = 13.749\text{Å}}$$

Sample b(900^oC for 10hrs):

For the peak(110) at $2\theta = 35.688^o$:

$$d = 2.5157\text{Å}$$

For this peak,

$$a = 2d$$
$$\implies \boxed{a = 5.0314\text{Å}}$$

For the peak(113) at $2\theta = 40.950^o$:

$$d = 2.2038\text{Å}$$

We have already calculated

$$a = 5.0314\text{Å}$$

Using this,

$$\implies \boxed{c = 13.710\text{Å}}$$

Lattice parameters according to the ICDD(International Centre for Diffraction Data) database: $a = b = 5.0356$Å, $c = 13.7489$Å, $\alpha = \beta = 90^o$ and $\gamma = 120^o$

4.5 Crystallite Size:

Using the Scherrer equation,

$$\beta(2\theta) = \frac{K\lambda}{L\cos\theta}$$

and taking $K = 0.94$ and $\lambda = 1.5417$Å,
crystallite sizes were calculated for the top intensity peaks with $2\theta \approx 30 - 50^o$

Table 4: FWHM and Crystallite size(Sample a)

Peak position $2\theta(^o)$	FWHM $\beta(^o)$	L (nm)
33.201	0.30944	28.002
35.688	0.31006	28.134
49.547	0.33033	27.686
54.166	0.37120	25.125

Average crystallite size for sample a= 27.237 nm

Table 5: FWHM and Crystallite size(Sample b)

Peak position $2\theta(^o)$	FWHM $\beta(^o)$	L (nm)
33.233	0.19914	43.515
35.687	0.21746	40.115
54.212	0.24885	37.486

Average crystallite size for sample b= 40.372 nm

Table 6: FWHM and Crystallite size(Sample c)

Peak position $2\theta(^o)$	FWHM $\beta(^o)$	L (nm)
33.004	0.29786	29.076
35.469	0.29407	29.646
49.357	0.31619	28.902
53.942	0.36886	25.26

Average crystallite size for sample c= 28.221 nm

Table 7: FWHM and Crystallite size(Sample d)

Peak position $2\theta(^o)$	FWHM $\beta(^o)$	L (nm)
33.139	0.26143	33.139
35.587	0.27233	32.023
40.831	0.21835	40.578
49.461	0.27266	33.53
54.091	0.3057	30.50

Average crystallite size for sample d= 33.954 nm

5 Results and Discussion

5.1 Characterization and XRD results

The diffractograms(powder XRD patterns) of both the samples were compared with the data from ICDD(International Centre for Diffraction Data) formerly JCPDS(Joint Committee for Powder Diffraction Studies) to index the peaks. The samples matched with JCPDS PDF(Powder Diffraction File) Card 33-0664 perfectly. The manual and rather tedious way of indexing the peaks of a hexagonal structure would be with the help of Hull-Davey diagrams. This was not feasible due to it's complexity. Had, the sample been of a simple structure like a cubic one, then the peaks could have been indexed using the ratios of the $\sin^2\theta$ terms. All the samples were phase pure as the XRD didn't show any trace of any other iron oxide like the β, γ or δ phase. The powder XRD pattern was also in good agreement with the simulated XRD pattern(done using VESTA) of our structure shown in figure 6. The calculated lattice parameters were also found to be in good agreement with ICDD database.
There are a few important things to note here:

- In contrast to the single-crystal diffraction, in the powder diffraction, reflections from planes of same interplanar spacing d_{hkl} are superimposed over each other, resulting in overlapping of peaks. This concept is also known as equivalent reflections. Thus, one can attach a multiplicity to the planes, telling the number of equivalent reflections corresponding to the hkl values. Multiplicity only occurs in powder diffraction, and so is not commonly discussed in connection with single-crystal data.
- It's already been stated, that the peak height largely, depends upon the number of atoms in a plane. Consequently, we should have observed the 110 peak to be the highest, as one can see in figure, that the number of atoms in this plane is really large. But, interestingly, the 104 peak was higher than the 110 peak indicating a preferential orientation of the crystals. Preferred orientation would cause a lot of crystals in the powder to lie in a particular orientation about a plane, leading to more number of reflections for that plane, and hence a higher peak.

The various planes observed in the XRD pattern have been shown below:

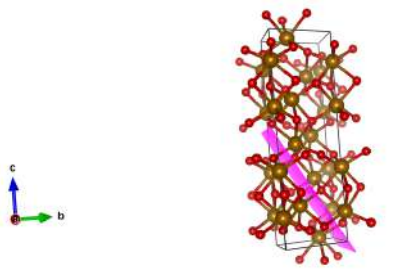

Figure 17: 012 Plane

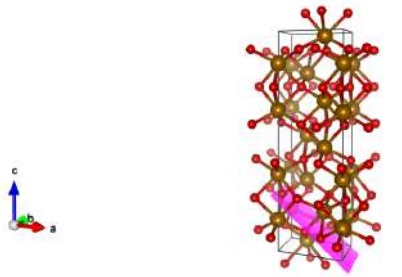

Figure 18: 104 Plane

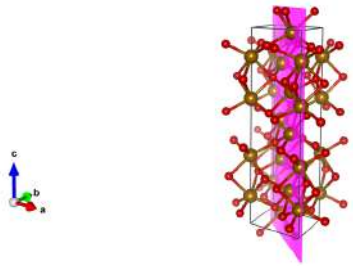

Figure 19: 110 Plane

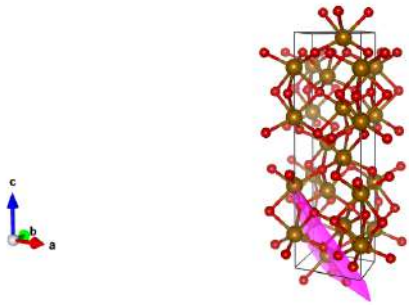

Figure 20: 113 Plane

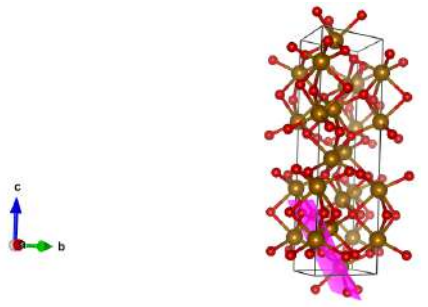

Figure 21: 024 Plane

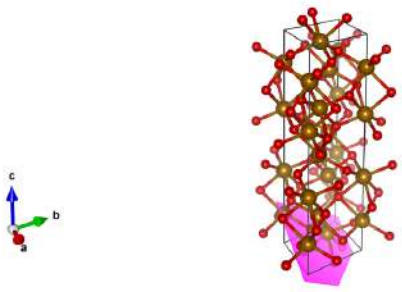

Figure 22: 116 Plane

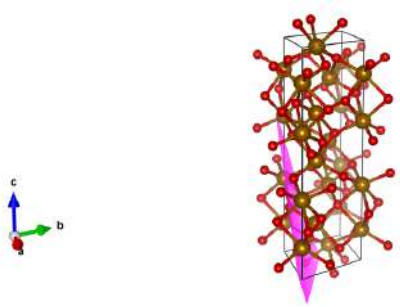

Figure 23: 122 Plane

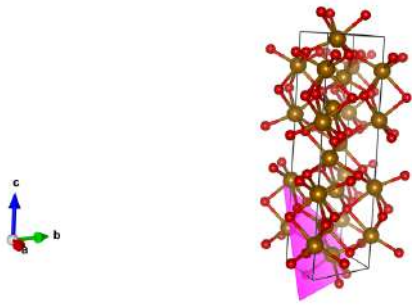

Figure 24: 214 Plane

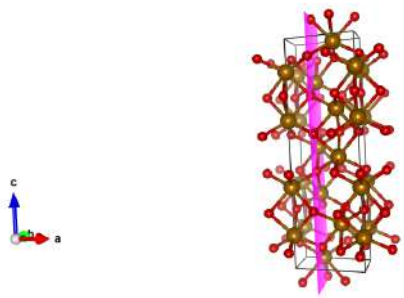

Figure 25: 300 Plane

5.2 Temperature dependence of Crystallite Size

Crystallite size was observed to increase with temperature. The sample prepared at 550^oC had a crystallite size of **27.237 nm** and the sample prepared at 900^oC had a crystallite size of **40.372 nm**. This was expected as literature reports indicated that the morphologies of α-Fe_2O_3 nanoparticles depend not only on the precursors, but also on the synthesis conditions and the annealing temperature.
However, the expected crystallite sizes of the samples were a little smaller than expected. This could be due to the following factors:

- The instrumental peak profile wasn't subtracted from the XRD pattern, therefore the the broadening term was large resulting in smaller calculated sizes. The instrumental peak profile could have been taken care of by preparing a standard sample larger than 200nm, and obtaining it's XRD pattern. The broadening due to such a huge crystallite size would be really small, and one could consider the broadening to be solely due to the instrument. This could then be subtracted from the XRD patterns.
- Peak broadening is also caused by micro strains in the material which haven't been considered in our discussion and calculations. Therefore, the crystallite sizes should only be taken as a **qualitative** measure of the dependence of size on temperature. For a better quantitative measure, TEM might be done.

The change in the reaction temperature influences the morphology and structure of nanomaterials because particle morphology is strongly dependent upon the supersaturation which in turn is dependent upon the solution temperature. The heat treatment has a predominant effect upon the grain growth. The reduction in the overall surface energy is the true driving force for the grain boundary enlargement and consequently the particle size increases as a function of the temperature. These results may be explained by the nucleation and growth of particles in a solution. Particle morphology is influenced by the factors such as supersaturation, nucleation and growth rates, colloidal stability, recrystallization and aging process. Generally, supersaturation, which is highly dependent on solution temperature, has a predominant influence on the morphology of the precipitates. A highly supersaturated solution possesses high Gibbs free energy. The tendency of a system to lower its Gibbs free energy is the driving force in the processes of nucleation and growth of particles.

5.3 Color of the samples

The colors of both the samples were different too.

- Sample prepared at 550^o C and calcinated for 20 hrs was **REDDISH BROWN** in color.
- Sample prepared at 900^o C and calcinated for 10 hrs was **METALLIC GREY** in color.

This could be largely attributed to the widening of band gap due to the different sizes of the samples. It's known, that the band gap increases with confinement(decrease in size). There are a lot of other factors too that affect the color of the crystals.

References

[1] Monika Sharma, Azeem Banday, and Sevi Murugavel, 2016
Size dependent polaronic conduction in hematite
doi: `http://dx.doi.org/10.1063/1.4948070`

[2] CIF File, *Blake R L, Hessevick R E, Zoltai T, Finger L W*
American Mineralogist Crystal Structure Database 51 (1966) 123-129
. http://rruff.geo.arizona.edu/AMS/download.php?id=00230.am&down=amc

[3] Scherrer Equation, *P. Scherrer, Bestimmung der Grsse und der inneren Struktur von Kolloidteilchen mittels Rntgenstrahlen, Nachr. Ges. Wiss. Gttingen 26 (1918) pp 98-100*

[4] JCPDS PDF 33-0664 for $\alpha - Fe_2O_3$ Card,
http://comptech.compres.us/tools/jcpds/Oxides/Fe2O3.jcpds

[5] VESTA, Visualizing Software,
http://jp-minerals.org/vesta/en/

[6] YouTube Tutorial,
https://www.youtube.com/watch?v=PwCc4ecj2w0&t=20s

[7] B. Levy, Photochemistry of nanostructured materials for energy applications",
Journal of Electroceramics, vol. 1, no. 3, pp. 239272, 1997.

[8] Chauhan P, Annapoorni S and Trikha S K 1999,
Thin Solid Films

[9] Fukazawa M, Matuzaki H and Hara K 1993,
Sensors Actuators

[10] Materialsproject.org 10.17188/1200378,
https://materialsproject.org/materials/mp-24972/

[11] A brief explanation of XRD on my blog,
http://www.bragitoff.com/2017/08/x-ray-diffraction-xrd/

[12] Frequently asked questions on XRD(blog link),
http://www.bragitoff.com/2017/08/faq-x-ray-diffraction-viva-questions/